A trajectory tracking control design for a skid-steering mobile robot by adapting its desired instantaneous center of rotation

Jae-Yun Jun, Minh Duc Hua, Faïz Ben Amar

A trajectory tracking control design for a skid-steering mobile robot by adapting its desired instantaneous center of rotation

Jae-Yun Jun, Minh-Duc Hua, Faïz Benamar

***Abstract*—A skid-steering mobile robot steers by creating a moment that is larger than the frictional moment which results in a lateral slippage also known as skidding. This moment is in turn generated by a difference of the forces originated from the two sides of the robot. Tracking a given trajectory using this type of steering mechanism is not easy since it requires to relate skidding to steering. A necessary condition for the stability of skid-steering mobile robots is that the longitudinal component of the instantaneous center of rotation (ICR) resides within the robot dimension. In the present work, we propose a novel trajectory-tracking control design using a backstepping technique that guarantees the Lyapunov stability and that satisfies this necessary condition by relating the longitudinal component of the "desired ICR" to the curvature of a given trajectory and the reference linear speed. Finally, we compare the performance of the proposed controller to that of other existing controllers for skid-steering mobile robots and show the robustness of the proposed controller even in the presence of modeled sensory noise and control time delay in simulation.**

I. Introduction

Skid-steering mobile robots are often used for their robustness owing to their simplicity. These robots steer by causing lateral skidding, which is the product of generating a difference in forces originated from the two sides of the robot. This difference creates a moment, and if this moment is larger than the frictional moment, then skidding takes place and, consequently, rotational motion. However, tracking a given trajectory using this type of steering mechanism is not easy because it is not straightforward to relate the necessary amount of skidding to accomplish a desired steering effect.

A first approach to establish the *skid-to-steer relationship* might be the search for the instantaneous pivot point in the world about which the moment is generated. This pivot point is also known as the *instantaneous center of rotation (ICR)*. The ICR can then be defined as the point in the world from which the robot's motion is viewed as a pure rotational motion. In other words, the ICR is the point in the world for which all the vectors that point to the contact points are perpendicular to their respective contact velocity vectors. As a result, one can deduce that, for this type of robots, the ICR is always away from their lateral axis that passes through their center of gravity when they make turns, and, therefore, skidding takes place.

Hence, the knowledge of the ICR location seems to make the skid-to-steer relationship hold. In the literature, there are several works on estimating the location of the ICR while a four-wheel skid-steering mobile robot [1] or a tracked mobile robot [2], with the purpose to improve the control of these types of robots. However, estimating the location of the ICR is not straightforward because it depends on the robot's instantaneous lateral velocity and its instantaneous angular velocity. Instead, one might be able estimate the longitudinal component of the "*desired ICR*" in the robot body coordinate system in order to generate steering motion while satisfying the robot stability.

In effect, there have been works on controlling the steering motion of four-wheel skid-steering mobile robots by forcing the desired ICR to be at a constant distance from the robot's center of gravity along the longitudinal axis [3], [4], where this distance is smaller than the longitudinal robot dimension in order to guarantee the controllability [3], [5]. This is achieved by establishing an operational nonholonomic constraint associated with the desired ICR location and by designing controllers that work to preserve this condition.

Despite the fact that this approach guarantees both the non-zero lateral velocity condition (and, therefore, skidding and in turn steering motion) and the controllability, for a given trajectory, a controller designed based on this approach might not be able to guarantee the asymptotic convergence in the error dynamics because the velocity relationship established by this operational nonholonomic constraint might not hold from the reference trajectory side.

In the present work, on top of the dynamic modeling of a planar four-wheel skid-steering mobile robot that *Caracciolo et al.* developed in [3], we propose a novel nonlinear trajectory-tracking controller that preserves the dynamics of the system, using a backstepping technique that guarantees the Lyapunov stability. Within this framework, we propose a method that sets the longitudinal component of the desired ICR as a function of the curvature of a given trajectory and the reference linear speed. As a result, we show that the controller proposed in the present work is more robust than the controller proposed in [3] even in the presence of sensory noise and control time delay.

The paper is organized as follows. In Section II, the dynamic modeling of a four-wheel skid-steering mobile robot is recalled and discussed. In Section III, a new operational nonholonomic constraint is proposed. In Section IV, a novel backstepping-based controller that guarantees the Lyapunov-stability is presented. In Section V, simulation results are reported and discussed. Finally, conclusion remarks and perspectives are given in Section VI.

Jae-Yun Jun, Minh-Duc Hua and Faïz Benamar are with:
1. Sorbonne Universités, UPMC Univ Paris 06, UMR 7222, ISIR, F-75005, Paris, France
2. CNRS, UMR 7222, ISIR, F-75005, Paris, France
e-mail: jaeyunjk@gmail.com, hua@isir.upmc.fr, amar@isir.upmc.fr

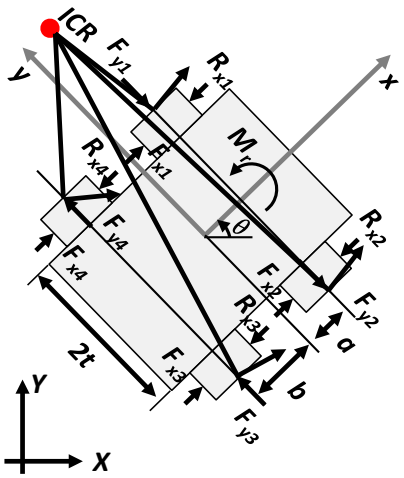

Fig. 1. A model for a four-wheel skid-steering mobile robot.

II. Recall on the dynamic modeling of a four-wheel skid-steering mobile robot

As shown in [3], the equations of motion of a four-wheel skid-steering mobile robot are given by

$$\mathbf{M}\ddot{\mathbf{q}} + \mathbf{c}(\mathbf{q}, \dot{\mathbf{q}}) = \mathbf{E}(\mathbf{q})\boldsymbol{\tau}, \tag{1}$$

where $\mathbf{q} \triangleq [X, Y, \theta]^T$ with (X, Y) the coordinates of the robot's center of mass expressed in the inertial frame and θ its yaw angle. The terms $\mathbf{M}$, $\mathbf{c}$ and $\mathbf{E}$ and the control vector $\boldsymbol{\tau}$ are defined as

$$\mathbf{M} \triangleq \begin{bmatrix} m & 0 & 0 \\ 0 & m & 0 \\ 0 & 0 & I \end{bmatrix}, \quad \mathbf{c}(\mathbf{q}, \dot{\mathbf{q}}) \triangleq \begin{bmatrix} R_x \cos\theta - F_y \sin\theta \\ R_x \sin\theta + F_y \cos\theta \\ M_r \end{bmatrix},$$
$$\mathbf{E}(\mathbf{q}) \triangleq \begin{bmatrix} \cos\theta/r & \cos\theta/r \\ \sin\theta/r & \sin\theta/r \\ t/r & -t/r \end{bmatrix}, \quad \tau_i = 2rF_{x_i}, \quad i = 1, 2$$

where m, I and r denote the robot's mass, its inertia about the body z-axis and the wheel radius, respectively. a, b and t are the robot's dimensional parameters (as defined in Fig. 1). F_{x_i} is the i-th wheel's tractive force. R_x, F_y and M_r are the resistive longitudinal and lateral forces, and the resistive moment, respectively, which can be computed as follows

$$\begin{aligned} R_x &= \sum_{i=1}^{4} R_{xi} = f_r \frac{mg}{2} \left(\text{sgn}(\dot{x}_1) + \text{sgn}(\dot{x}_2)\right), \\ F_y &= \sum_{i=1}^{4} F_{yi} = \mu \frac{mg}{a+b} \left(b\,\text{sgn}(\dot{y}_1) + a\,\text{sgn}(\dot{y}_3)\right), \\ M_r &= a(F_{y1} + F_{y2}) - b(F_{y3} + F_{y4}) \\ &\quad + t\left[(R_{x2} + R_{x3}) - (R_{x1} + R_{x4})\right] \\ &= \mu \frac{a\,b\,m\,g}{a+b} \left(\text{sgn}(\dot{y}_1) - \text{sgn}(\dot{y}_3)\right) \\ &\quad + f_r \frac{t\,m\,g}{2} \left(\text{sgn}(\dot{x}_2) - \text{sgn}(\dot{x}_1)\right), \end{aligned}$$

with g, f_r, μ, and $\text{sgn}(\cdot)$ the gravitational acceleration, the coefficient of rolling friction, the coefficient of lateral friction and the sign function, respectively. Besides, $\dot{x}_i$ and $\dot{y}_i$, with $i = 1, \cdots, 4$, are respectively the longitudinal and the lateral wheel velocities, subject to the following relationships with the linear and angular velocities $(\dot{x}, \dot{y}, \dot{\theta})$ expressed in the body frame

$$\begin{cases} \dot{x}_1 = \dot{x}_4 = \dot{x} - t\dot{\theta}, \\ \dot{x}_2 = \dot{x}_3 = \dot{x} + t\dot{\theta}, \\ \dot{y}_1 = \dot{y}_2 = \dot{y} + a\dot{\theta}, \\ \dot{y}_3 = \dot{y}_4 = \dot{y} - b\dot{\theta}. \end{cases}$$

The velocity in the body frame is related to the velocity in the inertial frame as follows

$$\begin{bmatrix} \dot{X} \\ \dot{Y} \end{bmatrix} = \mathbf{R} \begin{bmatrix} \dot{x} \\ \dot{y} \end{bmatrix}, \tag{2}$$

with $\mathbf{R} \triangleq \begin{bmatrix} \cos\theta & -\sin\theta \\ \sin\theta & \cos\theta \end{bmatrix}$ the rotation matrix.

III. New operational nonholonomic constraint

The location $(x_{\text{ICR}}, y_{\text{ICR}})$, expressed in the body frame, of the instantaneous center of rotation (ICR) should remain inside the robot's dimension along the longitudinal direction (i.e., $-b \leq x_{\text{ICR}} \leq a$) at any time instant in order to ensure the robot's motion stability. If the ICR goes outside the robot's dimension along the longitudinal direction, then all the resistive lateral forces F_{yi}, with $i = 1, \cdots, 4$, will have the same sign (equivalently all four lateral wheel speeds will have the same sign), and, consequently, there will be no way to balance the amount of skidding with the wheel actuators, causing the loss of controllability of the mobile robot [6]. If the location of the ICR is known, then a controller may be designed to track a reference trajectory while ensuring the constraint $-b \leq x_{\text{ICR}} \leq a$ so as to avoid instability. However, it is not easy to design such a controller due to the fact that the ICR is a function of the robot states, $[x_{\text{ICR}}, y_{\text{ICR}}] = [-\dot{y}/\dot{\theta}, \dot{x}/\dot{\theta}]$. A practical solution has been proposed by *Caracciolo et al.* [3] by imposing a "virtual" constraint $x_{\text{ICR}} = d_0$, with $0 < d_0 < a$. This yields the following nonholonomic constraint

$$\dot{y} + d_0\dot{\theta} = 0, \tag{3}$$

which implies that the lateral speed and the angular velocity should have a fixed relationship by the constant distance d_0. This "unnatural" constraint is not always satisfied in reality, and a controller should be designed to closely maintain this relationship.

Moreover, given a reference trajectory, both its curvature and the desired velocity might vary, and, therefore, (3) might not be adequate if the value for d_0 is fixed a priori. Under this hypothesis, a new operational nonholonomic constraint is proposed in the present work. which takes into account both the instantaneous curvature of a given trajectory and the desired linear speed. In fact, for a given trajectory, its expected centripetal acceleration is defined as

$$\hat{a}_y = \kappa(t)h(t), \tag{4}$$

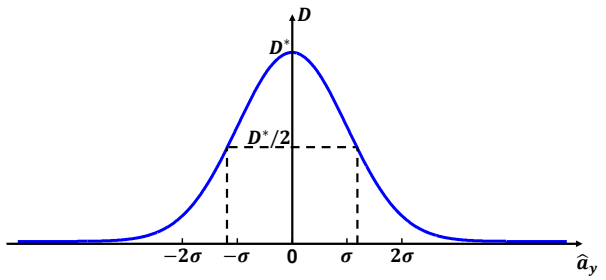

Fig. 2. The desired ICR along the longitudinal direction of the robot as function of the expected centripetal acceleration given from the reference trajectory.

where $h(t)$ is defined as $\dot{\boldsymbol{\xi}}_r^{\mathrm{T}}\dot{\boldsymbol{\xi}}_r$. In turn, $\dot{\boldsymbol{\xi}}_r = \left[\dot{\bar{X}}_r, \dot{\bar{Y}}_r\right]^{\mathrm{T}}$ represents the desired velocity of the control point for a given reference trajectory in the inertial frame. The control point is posteriorly defined in (15).

On the other hand, $\kappa(t)$ is the curvature of the trajectory and is defined as

$$\kappa = \frac{\dot{\bar{X}}_r\ddot{\bar{Y}}_r - \ddot{\bar{X}}_r\dot{\bar{Y}}_r}{\left(\dot{\bar{X}}_r^{\,2} + \dot{\bar{Y}}_r^{\,2}\right)^{3/2}}. \tag{5}$$

Let us now define the longitudinal component of the desired ICR as the constraint $x_{\mathrm{ICR}} = D$, where

$$D = D^* e^{-\frac{(\hat{a}_y))^2}{2\sigma^2}}, \tag{6}$$

in which D^* is a positive real value that represents $\max D$, and σ is a positive real number that represents the sensitivity of the modulation of D as function of κ and h. That is, the smaller σ is, the faster D approaches to small values (therefore, D is sensitive in the changes of the expected centripetal acceleration). However, the larger σ is, the more slowly D changes (therefore, D is less sensitive in the changes of the expected centripetal acceleration).

In essence, D has the form of a bell-shaped function as shown in Fig. 2 and depends on two terms: the curvature of a given trajectory and the squared reference linear speed. When the curvature (the reference linear speed) is small, the desired ICR point is moved as forward as possible (but bounded by the robot longitudinal dimension). But, when the curvature (the reference linear speed) is large, the desired ICR point is brought close to the center of gravity. D ranges between 0 and a.

Hence, (3) now becomes as

$$\dot{y} + D\dot{\theta} = 0. \tag{7}$$

Next, the first and the second time-derivatives of D can be computed as

$$\begin{aligned} \dot{D} &= -\frac{\hat{a}_y\dot{\hat{a}}_y}{\sigma^2}D, \\ \ddot{D} &= -\frac{1}{\sigma^2}\left[\left(\dot{\hat{a}}_y^2 + \hat{a}_y\ddot{\hat{a}}_y\right)D - \hat{a}_y\dot{\hat{a}}_y\dot{D}\right], \end{aligned} \tag{8}$$

where $\dot{\hat{a}}_y$ depends on $(h, \dot{h}, \kappa, \dot{\kappa})$, and $\ddot{\hat{a}}_y$, $(h, \dot{h}, \ddot{h}, \kappa, \dot{\kappa}, \ddot{\kappa})$. $\dot{h}$ and $\ddot{h}$ can be easily computed by differentiating h with respect to t and have as their expressions $2\dot{\boldsymbol{\xi}}_r^{\mathrm{T}}\ddot{\boldsymbol{\xi}}_r$ and $2\left(\ddot{\boldsymbol{\xi}}_r^{\mathrm{T}}\ddot{\boldsymbol{\xi}}_r + \dot{\boldsymbol{\xi}}_r^{\mathrm{T}}\dddot{\boldsymbol{\xi}}_r\right)$, respectively. Finally, $\dot{\kappa}$ and $\ddot{\kappa}$ can be easily computed by differentiating (5) with respect to time.

Inspired by [3], the system (1) is augmented by including the new operational nonholonomic constraint (7) as follows

$$\mathbf{M}\ddot{\mathbf{q}} + \mathbf{c}(\mathbf{q}, \dot{\mathbf{q}}) = \mathbf{E}(\mathbf{q})\boldsymbol{\tau} + \mathbf{A}(\mathbf{q})^{\mathrm{T}}\boldsymbol{\lambda}, \tag{9}$$

where $\boldsymbol{\lambda}$ is a vector of Lagrangian multipliers representing the constrained forces, while the matrix $\mathbf{A}$ holds the following relationship

$$\begin{bmatrix} -\sin\theta & \cos\theta & D \end{bmatrix}\begin{bmatrix} \dot{X} \\ \dot{Y} \\ \dot{\theta} \end{bmatrix} = \mathbf{A}(\mathbf{q})\dot{\mathbf{q}} = 0.$$

The admissible generalized velocities $\dot{\mathbf{q}}$ can be defined as

$$\dot{\mathbf{q}} = \mathbf{N}(\mathbf{q})\boldsymbol{\eta}, \tag{10}$$

where $\boldsymbol{\eta} \in \mathbb{R}^2$ is a pseudo-velocity, and the columns of the matrix $\mathbf{N}$ are in the null space of $\mathbf{A}$, e.g.,

$$\mathbf{N}(\mathbf{q}) = \begin{bmatrix} \cos\theta & -\sin\theta \\ \sin\theta & \cos\theta \\ 0 & -\frac{1}{D} \end{bmatrix}.$$

By differentiating (10) and eliminating $\boldsymbol{\lambda}$ from (9) one obtains

$$\begin{cases} \dot{\mathbf{q}} = \mathbf{N}\boldsymbol{\eta}, \\ \mathbf{N}^{\mathrm{T}}\mathbf{M}\mathbf{N}\dot{\boldsymbol{\eta}} = \mathbf{N}^{\mathrm{T}}(\mathbf{E}\boldsymbol{\tau} - \mathbf{M}\dot{\mathbf{N}}\boldsymbol{\eta} - \mathbf{c}). \end{cases} \tag{11}$$

One verifies that the matrices $\mathbf{N}^{\mathrm{T}}\mathbf{M}\mathbf{N}$ and $\mathbf{N}^{\mathrm{T}}\mathbf{E}$ are invertible. Thus, by making simple change of control variables

$$\boldsymbol{\tau} = \left(\mathbf{N}^{\mathrm{T}}\mathbf{E}\right)^{-1}\left(\mathbf{N}^{\mathrm{T}}\mathbf{M}\mathbf{N}\mathbf{u} + \mathbf{N}^{\mathrm{T}}\mathbf{M}\dot{\mathbf{N}}\boldsymbol{\eta} + \mathbf{N}^{\mathrm{T}}\mathbf{c}\right), \tag{12}$$

with $\mathbf{u} = \begin{bmatrix} u_1 & u_2 \end{bmatrix}^{\mathrm{T}}$ the vector of new control variables, then system (11) can be rewritten as

$$\begin{cases} \dot{\mathbf{q}} = \mathbf{N}\boldsymbol{\eta}, \\ \dot{\boldsymbol{\eta}} = \mathbf{u}, \end{cases} \tag{13}$$

which is equivalent to

$$\begin{cases} \dot{X} = \cos\theta\eta_1 - \sin\theta\eta_2, \\ \dot{Y} = \sin\theta\eta_1 + \cos\theta\eta_2, \\ \dot{\theta} = -\dfrac{1}{D}\eta_2, \\ \dot{\eta}_1 = u_1, \\ \dot{\eta}_2 = u_2. \end{cases} \tag{14}$$

IV. A Novel Trajectory Tracking Control Design Based on a Backstepping Procedure that Guarantees the Lyapunov Stability

A. Control design

Similar to [3], a control point is chosen on the longitudinal body axis at the distance D from the origin of the body frame. But, in the present work, the control point is modulated as described in Section III. Notice that the controller is designed for the system (14).

The vector of coordinates expressed in the inertial frame of this control point is thus given by

$$\boldsymbol{\xi} = \begin{bmatrix} \bar{X} \\ \bar{Y} \end{bmatrix} = \begin{bmatrix} X + D\cos\theta \\ Y + D\sin\theta \end{bmatrix}. \tag{15}$$

From (14), one verifies that the time-derivative of $\boldsymbol{\xi}$ satisfies

$$\dot{\boldsymbol{\xi}} = \eta_1 \mathbf{R}\mathbf{e}_1, \quad \text{with} \quad \mathbf{e}_1 \triangleq \begin{bmatrix} 1 & 0 \end{bmatrix}^{\mathrm{T}}.$$

Let $\boldsymbol{\xi}_r \in \mathbb{R}^2$ denote the reference position expressed in the inertial frame for the control point defined up to third-order derivative. Define $\tilde{\boldsymbol{\xi}} \triangleq \boldsymbol{\xi} - \boldsymbol{\xi}_r$ and $\bar{\boldsymbol{\xi}} \triangleq \mathbf{R}^{\mathrm{T}}\tilde{\boldsymbol{\xi}}$ as the position errors expressed in the inertial frame and body frame, respectively.

It is straightforward to deduce following equations of the error dynamics

$$\begin{cases} \dot{\bar{\boldsymbol{\xi}}} = -\omega\mathbf{S}\bar{\boldsymbol{\xi}} + \eta_1\mathbf{e_1} - \mathbf{R}^{\mathrm{T}}\dot{\boldsymbol{\xi}}_r, \\ \dot{\mathbf{R}} = \omega\mathbf{R}\mathbf{S}, \\ \dot{\eta}_1 = u_1, \\ \dot{\omega} = \bar{u}_2, \end{cases} \tag{16}$$

with $\bar{u}_2 \triangleq \frac{\dot{D}}{D^2}\eta_2 - \frac{1}{D}u_2$ the new control variable, $\omega \triangleq \dot{\theta}$ and $\mathbf{S} \triangleq \begin{bmatrix} 0 & -1 \\ 1 & 0 \end{bmatrix}$. Then, the control objective can be stated as the asymptotical stabilization of $\bar{\boldsymbol{\xi}}$, or equivalently of $\tilde{\boldsymbol{\xi}}$, about zero using $(u_1, \bar{u}_2)$ as control inputs.

The first equation of (16) indicates that the relation $\bar{\boldsymbol{\xi}} \equiv \mathbf{0}$ implies that

$$\eta_1\mathbf{e_1} - \mathbf{R}^{\mathrm{T}}\dot{\boldsymbol{\xi}}_r \equiv \mathbf{0}. \tag{17}$$

As long as $|\dot{\boldsymbol{\xi}}_r|$ is different from zero, one can define a locally unique solution of $\mathbf{R}$ (or θ) to equation (17). However, this solution cannot be prolonged by continuity at $\dot{\boldsymbol{\xi}}_r = \mathbf{0}$. This singularity corresponds to the case when the linearization of system (16) at any equilibrium $(\bar{\boldsymbol{\xi}}, \mathbf{R}, \omega) = (\mathbf{0}, \mathbf{R}^*, 0)$ is not controllable. Moreover, one can verify from the application of the Brockett's theorem [7] for this case that there does not exist any time-invariant $\mathcal{C}^1$ feedback control law that asymptotically stabilizes the system at the equilibrium $(\bar{\boldsymbol{\xi}}, \mathbf{R}, \omega) = (\mathbf{0}, \mathbf{R}^*, 0)$. We thus discard this difficult issue in the present work and make the following assumption with the purpose to propose a trajectory tracking control design based on a backstepping technique that guarantees the Lyapunov stability,

Assumption 1. *There exist positive constants δ_r and a_r such that $|\dot{\boldsymbol{\xi}}_r(t)| \geq \delta_r$ and $|\ddot{\boldsymbol{\xi}}_r(t)| \leq a_r$, $\forall t$.*

The following result is obtained based on a Lyapunov function constructed using a backstepping proceduce.

Proposition 1. *Consider the error system* (16)*. Assume that Assumption 1 holds. Let η_{1d} and ω_d denote auxiliary control variables derived from the backstepping procedure and defined as*

$$\begin{cases} \eta_{1d} \triangleq \mathbf{e}_1^{\mathrm{T}}\mathbf{R}^{\mathrm{T}}\dot{\boldsymbol{\xi}}_r - k_1\bar{\xi}_1, \\ \omega_d \triangleq \omega_r - k_2|\dot{\boldsymbol{\xi}}_r|\bar{\xi}_2 + k_3|\dot{\boldsymbol{\xi}}_r|\left(\mathbf{e}_2^{\mathrm{T}}\mathbf{R}^{\mathrm{T}}\dot{\boldsymbol{\xi}}_{\mathbf{r}}\right), \end{cases} \tag{18}$$

where $\omega_r \triangleq -\frac{\dot{\boldsymbol{\xi}}_{\mathbf{r}}^{\mathrm{T}}\mathbf{S}\ddot{\boldsymbol{\xi}}_{\mathbf{r}}}{|\dot{\boldsymbol{\xi}}_{\mathbf{r}}|^2}$, $k_{1,2}$ are positive constant gains, and k_3 is a positive gain (not necessarily constant) satisfying $\inf_t k_3(t) > 0$. Apply the following control law

$$\begin{cases} u_1 = \dot{\eta}_{1d} - k_4\bar{\xi}_1 - k_6(\eta_1 - \eta_{1d}), \\ \bar{u}_2 = \dot{\omega}_d + \dfrac{k_5}{k_2}\dfrac{\mathbf{e}_2^{\mathrm{T}}\mathbf{R}^{\mathrm{T}}\dot{\boldsymbol{\xi}}_{\mathbf{r}}}{|\dot{\boldsymbol{\xi}}_{\mathbf{r}}|} + \left(\dfrac{\dot{k}_5}{2k_5} - k_7\right)(\omega - \omega_d), \end{cases} \tag{19}$$

where $k_{4,6}$ are positive constant gains and $k_{5,7}$ are positive gains (not necessarily constant) satisfying $\inf_t k_{5,7}(t) > 0$. Then, the following properties hold:

1) *There exist only two equilibria $(\bar{\boldsymbol{\xi}}, \mathbf{R}, \omega) = (\mathbf{0}, \mathbf{R}_{\pm}^*, \omega_r)$, with $\mathbf{R}_+^{*\mathrm{T}}\mathbf{e}_1 = \frac{\dot{\boldsymbol{\xi}}_r}{|\dot{\boldsymbol{\xi}}_r|}$ and $\mathbf{R}_-^{*\mathrm{T}}\mathbf{e}_1 = -\frac{\dot{\boldsymbol{\xi}}_r}{|\dot{\boldsymbol{\xi}}_r|}$.*
2) *The equilibrium $(\bar{\boldsymbol{\xi}}, \mathbf{R}, \omega) = (\mathbf{0}, \mathbf{R}_+^*, \omega_r)$ is almost-globally asymptotically stable.*

Proof. The first property of Proposition 1 can be straightforwardly deduced from (16) and (17). We prove now the second property. Consider the following storage function

$$\mathcal{S} \triangleq \frac{1}{2}|\bar{\boldsymbol{\xi}}|^2 + \frac{1}{k_2}\left(1 - \frac{\mathbf{e}_1^{\mathrm{T}}\mathbf{R}^{\mathrm{T}}\dot{\boldsymbol{\xi}}_r}{|\dot{\boldsymbol{\xi}}_r|}\right), \quad (k_2 > 0) \tag{20}$$

whose time-derivative along the system's solutions satisfies (using Lemma 5 in [8])

$$\begin{aligned} \dot{\mathcal{S}} &= \bar{\boldsymbol{\xi}}^{\mathrm{T}}\left(\eta_1\mathbf{e_1} - \mathbf{R}^{\mathrm{T}}\dot{\boldsymbol{\xi}}_r\right) \\ &\quad + \frac{1}{k_2}\left(\frac{\omega\mathbf{e}_1^{\mathrm{T}}\mathbf{S}\mathbf{R}^{\mathrm{T}}\dot{\boldsymbol{\xi}}_r}{|\dot{\boldsymbol{\xi}}_r|} - \mathbf{e}_1^{\mathrm{T}}\mathbf{R}^{\mathrm{T}}\frac{d}{dt}\left(\frac{\dot{\boldsymbol{\xi}}_r}{|\dot{\boldsymbol{\xi}}_r|}\right)\right) \\ &= \bar{\xi}_1\left(\eta_1 - \mathbf{e}_1^{\mathrm{T}}\mathbf{R}^{\mathrm{T}}\dot{\boldsymbol{\xi}}_r\right) - \frac{\mathbf{e}_2^{\mathrm{T}}\mathbf{R}^{\mathrm{T}}\dot{\boldsymbol{\xi}}_r}{k_2|\dot{\boldsymbol{\xi}}_{\mathbf{r}}|}\left(\omega - \omega_r + k_2|\dot{\boldsymbol{\xi}}_{\mathbf{r}}|\bar{\xi}_2\right), \end{aligned}$$

with ω_r defined in Proposition 1. Then, using the expressions (18) of the auxiliary control variables η_{1d} and ω_d one deduces

$$\dot{\mathcal{S}} = -k_1\bar{\xi}_1^2 - \frac{k_3}{k_2}(\mathbf{e}_2^{\mathrm{T}}\mathbf{R}^{\mathrm{T}}\dot{\boldsymbol{\xi}}_{\mathbf{r}})^2 + \bar{\xi}_1(\eta_1 - \eta_{1d}) - \frac{\mathbf{e}_2^{\mathrm{T}}\mathbf{R}^{\mathrm{T}}\dot{\boldsymbol{\xi}}_{\mathbf{r}}}{|\dot{\boldsymbol{\xi}}_{\mathbf{r}}|}(\omega - \omega_d).$$

Now, backstepping procedure can be applied to deduce the real control inputs $(u_1, \bar{u}_2)$. Consider the following Lyapunov candidate function

$$\mathcal{L} \triangleq \mathcal{S} + \frac{1}{2k_4}\left(\eta_1 - \eta_{1d}\right)^2 + \frac{1}{2k_5}\left(\omega - \omega_d\right)^2, \tag{21}$$

with $\mathcal{S}$ defined by (20). From the system (16) and the control expressions (19), one deduces

$$\begin{aligned} \dot{\mathcal{L}} &= \dot{\mathcal{S}} + \frac{1}{k_4}\left(\eta_1 - \eta_{1d}\right)\left(u_1 - \dot{\eta}_{1d}\right) \\ &\quad + \frac{1}{k_5}(\omega - \omega_d)(\bar{u}_2 - \dot{\omega}_d) - \frac{\dot{k}_5}{2k_5^2}(\omega - \omega_d)^2 \\ &= -k_1\bar{\xi}_1^2 - \frac{k_3}{k_2}(\mathbf{e}_2^{\mathrm{T}}\mathbf{R}^{\mathrm{T}}\dot{\boldsymbol{\xi}}_r)^2 - \frac{k_6}{k_4}\left(\eta_1 - \eta_{1d}\right)^2 - \frac{k_7}{k_5}(\omega - \omega_d)^2 \end{aligned} \tag{22}$$

Since $\dot{\mathcal{L}}$ is negative semi-definite, the terms $\bar{\boldsymbol{\xi}}$, $\eta_1 - \eta_{1d}$ and $\omega - \omega_d$ remain bounded. From the boundedness of the reference acceleration $\ddot{\boldsymbol{\xi}}_{\boldsymbol{r}}$ (Assumption 1), one can show that

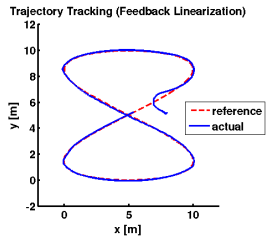

(a) Feedback linear. ($t_d = 10ms$)

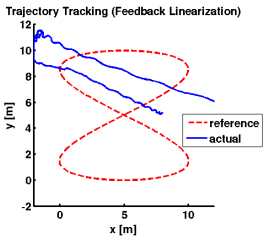

(b) Feedback linear. ($t_d = 20ms$)

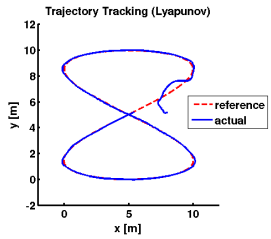

(c) Lyapunov with d_0 ($t_d = 10ms$)

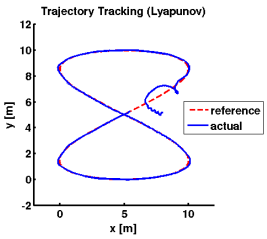

(d) Lyapunov with d_0 ($t_d = 20ms$)

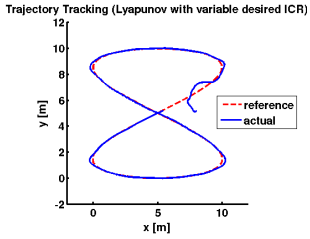

(e) Lyapunov with D ($t_d = 10ms$)

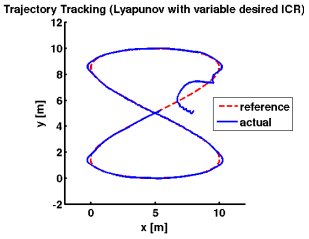

(f) Lyapunov with D ($t_d = 20ms$)

Fig. 3. The performance of the considered three controllers are compared while the robot model is asked to track an eight-shaped Lissajous curve trajectory defined in (27). In addition, a white Gaussian noise is added to the state vector to emulate the sensory noise. Moreover, two control delay time values ($t_d = \{10, 20\}$ ms) are considered to study the robustness of the controllers.

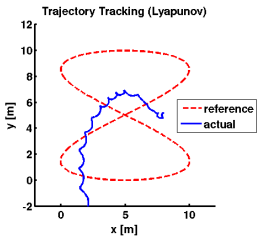

(a) Lyapunov with d_0 ($t_d = 30ms$)

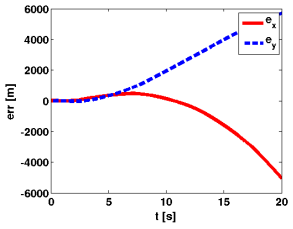

(b) Lyapunov with d_0 ($t_d = 30ms$)

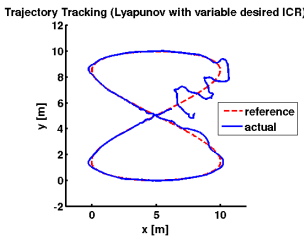

(c) Lyapunov with D ($t_d = 30ms$)

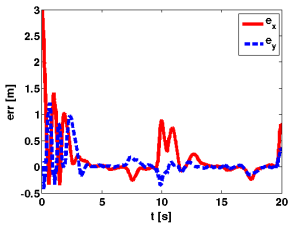

(d) Lyapunov with D ($t_d = 30ms$)

Fig. 4. The performance of the backstepping controllers with fixed desired ICR and variable desired ICR locations are compared for an eight-shaped Lissajous curve trajectory defined in (27). In addition, a white Gaussian noise is added to the state vector to emulate the sensory noise, and a control delay time of 30 ms is considered to study the robustness of the controllers. The tracking results and the error functions along the X- and Y-directions are shown.

$\ddot{\mathcal{L}}$ is bounded which implies that $\dot{\mathcal{L}}$ is uniformly continuous along every system's solution. Then, by the application of the Barbalat's lemma [9], one can ensure that $\dot{\mathcal{L}}$ converges to zero. Consequently, one can deduce that

$$\left(\bar{\xi}_1, \mathbf{e}_2^{\mathrm{T}}\mathbf{R}^{\mathrm{T}}\dot{\boldsymbol{\xi}}_r, \eta_1 - \eta_{1d}, \omega - \omega_d\right) \to \mathbf{0}. \tag{23}$$

In addition, one needs to make sure that $\bar{\xi}_2$ asymptotically converges to zero. If u_1 and $\bar{u}_2$ are defined as (19), then ω converges to ω_d as indicated in (23). Using this fact and the Lemma 5 of [8], one gets

$$\frac{d}{dt}\left(\frac{\mathbf{e}_2^{\mathrm{T}}\mathbf{R}^{\mathrm{T}}\dot{\boldsymbol{\xi}}_r}{|\dot{\boldsymbol{\xi}}_r|}\right) \to -\frac{\mathbf{e}_1^{\mathrm{T}}\mathbf{R}^{\mathrm{T}}\dot{\boldsymbol{\xi}}_r}{|\dot{\boldsymbol{\xi}}_r|}\left(\omega_d - \omega_r\right). \tag{24}$$

From (23), $\mathbf{e}_2^{\mathrm{T}}\mathbf{R}^{\mathrm{T}}\dot{\boldsymbol{\xi}}_r$ converges to zero. Therefore, the ω_d given in (18) converges to

$$\omega_d \to \omega_r - k_2|\dot{\boldsymbol{\xi}}_{\mathbf{r}}|\bar{\xi}_2. \tag{25}$$

Using (25) in (24), one gets

$$\frac{d}{dt}\left(\frac{\mathbf{e}_2^{\mathrm{T}}\mathbf{R}^{\mathrm{T}}\dot{\boldsymbol{\xi}}_r}{|\dot{\boldsymbol{\xi}}_r|}\right) \to k_2(\mathbf{e}_1^{\mathrm{T}}\mathbf{R}^{\mathrm{T}}\dot{\boldsymbol{\xi}}_r)\bar{\xi}_2. \tag{26}$$

On the other hand, since $\left(\mathbf{e_2^T R^T \dot{\xi}_r}\right) \to 0$ holds (from (23)), $\frac{d}{dt}\left(\mathbf{e_2^T R^T \dot{\xi}_r}\right) \to 0$ must be true. Using Assumption 1, $|\dot{\boldsymbol{\xi}}_{\mathbf{r}}| \neq 0$. Hence, $\frac{d}{dt}\left(\frac{\mathbf{e_2^T R^T \dot{\xi}_r}}{|\dot{\boldsymbol{\xi}}_{\mathbf{r}}|}\right) \to 0$ must also be true. Therefore, $\mathbf{e_1^T R^T \dot{\xi}_r} k_2 \bar{\xi}_2 \to 0$. But, $\mathbf{e_1^T R^T \dot{\xi}_r} \nrightarrow 0$, and $k_2 > 0$. Therefore, $\bar{\xi}_2 \to 0$. □

V. Results and Discussion

In this section, the performance of three trajectory tracking controllers are compared: the feedback linearization approach proposed in [3], the backstepping controller proposed in the present work with fixed control point, and the same as the latter one but with variable desired ICR location as shown in the previous section. The comparison is performed using the MATLAB/Simulink. For all three controllers, the system (1) is independently solved using MATLAB ode-solver of type *ode5 (Dormand-Prince)* with a fixed time step (5ms).

In the first place, the considered initial conditions are $x_o = 8$ m, $y_o = 5$ m, $\theta_o = \pi/2$ rad, $\dot{x}_o = 0.5$ m/s, $\dot{y}_o = 0.5$ m/s, $\dot{\theta}_o = 0.1$ rad/s. Next, the considered robot dimensions correspond to those of an ATRV-2 mobile robot used in [3] with $m = 116$ kg, $I = 20$ kgm^2, $a = 0.37$ m, $b = 0.55$ m, $t = 0.315$ m, $d_0 = 0.18$ m, and $r = 0.2$ m. For the controller proposed in the present work, the following parameter values are used: $D^* = a/2.5$ and $\sigma = 2$.

For a reasonable comparison between the three controllers, the gains are independently tuned for tracking a circular trajectory of 5 m radius. The resulting gains for the dynamic-feedback-linearization-based controller are $k_{v_1} = 131$, $k_{a_1} = 20$, $k_{p_1} = 325$, $k_{v_2} = 210$, $k_{a_1} = 67$, and $k_{p_1} = 580$. Whereas,

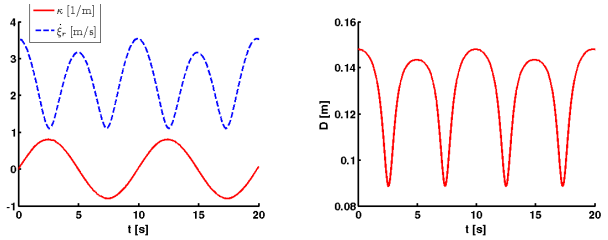

(a) Curvature and the desired linear speed (b) The longitudinal component of the desired ICR

Fig. 5. The curvature of the eight-shaped Lissajous curve trajectory defined in (27) and the reference linear speed are shown in (a). The longitudinal component of the desired ICR defined in (6) is shown for the considered Lissajous curve trajectory in (b).

for the Lyapunov-based controller, the resulting gains are $k_1 = 3$, $k_2 = 15.8$, $\kappa_3 = 7.95$, $k_4 = 1$, $\kappa_5 = 0.0005$, $k_6 = 5$, and $\kappa_7 = 4.05$.

Next, these gains are used to compare the performance of the three controllers in tracking an eight-shaped Lissajous-curve trajectory is considered as shown in Fig. 3 and Fig. 4. This trajectory is characterized by its curvature that continuously changes as shown in Fig. 5(a). The considered Lissajous curve has the following expression

$$\boldsymbol{\xi}_r = \begin{bmatrix} \bar{X}_r(t) \\ \bar{Y}_r(t) \end{bmatrix} = \begin{bmatrix} 5\left(1+\sin\left(\sqrt{0.4}t\right)\right) \\ 5\left(1+\sin\left(\sqrt{0.4}t/2\right)\right) \end{bmatrix}. \qquad (27)$$

Further, a multi-variate white Gaussian noise is added to the state vector to emulate the sensor noise and study the robustness of both controllers. The considered noise has the following mean and standard deviation values: $\mu_x = 0$ m, $\mu_y = 0$ m, $\mu_\theta = 0$ rad, $\mu_{\dot{x}} = 0$ m/s, $\mu_{\dot{y}} = 0$ m/s, $\mu_{\dot{\theta}} = 0$ rad/s, $\sigma_x = 0.02$ m, $\sigma_y = 0.02$ m, $\sigma_\theta = 0.01$ rad, $\sigma_{\dot{x}} = 0.08$ m/s, $\sigma_{\dot{y}} = 0.08$ m/s, and $\sigma_{\dot{\theta}} = 0.01$ rad/s.

Finally, on top of the additive noise, a control time delay is also considered to further study the robustness of the system controlled by each of the considered controllers. The results presented in Fig. 3 show the tracking performance for a control time delay of 10 ms and 20 ms. When the control delay time is 10 ms, all three controllers are able to track the trajectory (27). However, when the delay time is 20 ms, then the feedback linearization approach is unable to track the trajectory. We further increase the delay time to 30 ms for the backstepping approach with d_0 and D. Fig. 4 shows that the backstepping controller with d_0 fails to track the trajectory (27), but the controller proposed in the present work is able to track the trajectory.

Fig. 5 shows the curvature of the considered Lissajous function, the reference linear speed and the modulation of D as function of the aforementioned variables. One can see that as the curvature of the trajectory increases, both the reference linear speed and D decrease. The fact that the curvature increases implies that the robot is expected to make sharp turns, and, therefore, D should be close to the center of gravity in order not to lose the stability.

VI. Conclusion and Future Work

In the present work, a trajectory tracking control design is proposed for a planar four-wheel skid-steering mobile robot, using a backstepping technique that guarantees the Lyapunov stability and that maintains the longitudinal component of the ICR to be within the robot dimension. This purpose is achieved by defining the longitudinal component of the "desired ICR", which is a function of both the curvature of a given trajectory and the reference linear speed. The proposed controller is compared to other already-existing controllers for skid-steering mobile robots, and we show that the presented controller shows robustness in the presence of sensory noise and control time delay.

In the future, the proposed controller will be validated by implementing it on actual skid-steering mobile robots.

Acknowledgement

This work is partially supported by the RAPID-FRAUDO project (Num. 112906242) funded by the DGA (French Defence Agency).

References

[1] A. Mandow, J. L. Martínez, J. Morales, and J. L. Blanco, "Experimental kinematics for wheeled skid-steer mobile robots," in *Proc. of IEEE/RSJ International Conference on Intelligent Robots and Systems*, 2007.

[2] J. Martinez, A. M. andJ. Morales andS. Pedraza, and A. Garcia-Cerezo, "Approximating kinematics for tracked mobile robots," *International Journal of Robotics Research*, vol. 24, pp. 867–878, 2005.

[3] L. Caracciolo, A. De Luca, and S. Iannitti, "Trajectory tracking control of a four-wheel differentially driven mobile robot," in *Proc. of IEEE International Conference on Robotics and Automation*, vol. 4, 1999, pp. 2632–2638.

[4] K. Kozlowski and D. Pazderski, "Modeling and control of a 4-wheel skid-steering mobile robot," *International Journal of Applied Mathematics and Computer Science*, vol. 14, no. 4, pp. 477–96, 2004.

[5] Z. Shiller and W. Serate, "Trajectory planning of tracked vehicles," *Transactions of the ASME. Journal of Dynamic Systems, Measurement and Control*, vol. 117, no. 4, pp. 619–24, Dec. 1995.

[6] Z. Shiller, W. Serate, and M. Hua, "Trajectory planning of tracked vehicles," in *Proc. of IEEE International Conference on Robotics and Automation*, vol. 3, 1993, pp. 796–801.

[7] R. Brockett, "Asymptotic stability and feedback stabilization," *Differential geometric control theory*, pp. 181–191.

[8] M.-D. Hua, "Contributions au contrôle automatique de véhicules aériens," Ph.D. dissertation, Université de Nice-Sophia Antipolis, 2009.

[9] H. K. Khalil, *Nonlinear systems*, 2nd ed. Prentice-Hall, 1996.